01 Sep 2022

Effect of Rolling Process on Magnetic Properties of Fe-3.3 Wt% Si Non-Oriented Electrical Steel

Yizhou Du

Ronald J. O'Malley
Missouri University of Science and Technology, omalleyr@mst.edu

Mario F. Buchely
Missouri University of Science and Technology, buchelym@mst.edu

Paul Kelly

Recommended Citation

Y. Du et al., "Effect of Rolling Process on Magnetic Properties of Fe-3.3 Wt% Si Non-Oriented Electrical Steel," *Applied Physics A: Materials Science and Processing*, vol. 128, no. 9, article no. 765, Springer, Sep 2022.
The definitive version is available at https://doi.org/10.1007/s00339-022-05902-5

Applied Physics A (2022) 128: 765
https://doi.org/10.1007/s00339-022-05902-5

Applied Physics A
Materials Science & Processing

Effect of rolling process on magnetic properties of Fe-3.3 wt% Si non-oriented electrical steel

Yizhou Du[1,3] · Ronald J. O'Malley[1] · M. F. Buchely[1] · Paul Kelly[2]

Received: 6 January 2022 / Accepted: 27 July 2022 / Published online: 10 August 2022

Abstract

In this study, the influence of the rolling process on magnetic properties of Fe-3.3 wt% Si non-oriented electrical steel was investigated. The strip samples were cast using a high solidification cooling rate vacuum sampling method to simulate the solidification conditions of the industrial twin roll thin strip casting (TRSC) process. As-cast samples were subjected to various thermo-mechanical processing routes with different levels of hot-rolling (HR) and cold-rolling (CR). The influence of carbon and sulfur (C&S) contents in the steel were also investigated. Core loss ($P_{1.5/50}$, $P_{1.5/60}$, $P_{1.0/50}$, $P_{1.0/60}$) and magnetic induction (B_{25}, B_{50}) of the final annealed strip samples were measured to investigate how the magnetic properties are influenced by the final grain-size and texture. It was observed that increased HR deformation increased average final grain size after processing. This larger grain size resulted in lower core loss and higher magnetic induction. For the same level of HR deformation, low C&S steel compositions had exhibited a larger average grain size after the recrystallization annealing than high C&S steels. Using texture measurements, it was observed that the intensity of Goss orientation decreased with an increase in HR deformation.

Keywords Electric steel · Magnetic properties · Rolling process · Texture · Twin-roll thin strip casting

1 Introduction

Electrical steel is a low carbon iron–silicon soft magnetic alloy which is widely used in electric motors, sensors, power generators, and transformers. Electrical steels can be classified into non-grain-oriented (NGO) and grain-oriented (GO) electrical steels. Cold-rolled non-grain-oriented steel (CRNGO) is generally less expensive than cold-rolled grain-oriented steel (CRGO). Thus, when the cost is important, or when the direction of magnetic flux for the application is not constant, NGO electrical steel is used [1].

Based on the application, it is important to control the magnetic properties of the NGO electrical steel [2, 3]. The magnetic properties of the NGO electrical steel are highly influenced by the grain size and texture, which are in turn influenced by the rolling and recrystallization annealing processes [4, 5]. Park et al. reported that, after final annealing, 2.0 wt% Si NGO electrical steel has strong {110}⟨001⟩ (Goss) texture [6]. Lu, Yukuan et al. reported that, for 4.5 wt% Si NGO electrical steel, a two-step cold rolling can help to form coarse grains with a strong Goss and near Goss recrystallization texture in the annealing process [7].

The magnetic properties for electrical steels are highly influenced by the texture. In electrical steels, the <001> axis direction is easily magnetized, while the <111> axis direction is more difficult to magnetize. Goss and Cube orientations are ideal for magnetic properties [8, 9]. Brass and Goss orientations are reported to be formed in the BCC metals through shear deformation texture [10]. Many Goss grains and Cube grains are formed at the shear bands within the γ-fiber deformed regions [11]. Some Cube components are retained after the heavy cold rolling process because the Cube deformation bands also serve as the nucleation sites of the new Cube grains [8, 9].

For NGO electrical steel, it is difficult to control texture during the recrystallization annealing process. In some cases, a phase transformation is used to obtain the

✉ Yizhou Du
yd3t2@mst.edu

[1] Department of Materials Science and Engineering, Missouri S&T, 1400 N Bishop Avenue, Rolla, MO 65409-034, USA

[2] Consultant Castrip LLC, Charlotte, NC, USA

[3] MCC Capital Engineering and Research Incorporation Limited, Beijing, China

ideal orientation for magnetic properties. During the annealing process, because of anisotropic strain energy, some {100} oriented grains are formed when austenite transforms to ferrite [8, 9]. However, this method is not available for fully ferritic steel compositions. Thus, methods to achieve ideal crystallographic orientations with chemical compositions without a phase transformation has also been studied in literature [12, 13]. Pedrosa et al. reported the influence of initial annealing on texture evolution and magnetic properties for a 3.4 wt% Si electrical steel with 0.003 wt% C [14]. The recrystallization kinetics of a 3 wt% Si electrical steel were also studied [12].

The rolling process also has a significant influence on texture evolution, grain growth, and magnetic properties [12, 15]. In the annealing process, some ideal textures evolve from deformed shear bands which are formed by the rolling process [8]. Furthermore, the phase transformation during hot deformation also affects the recrystallization rate and grain size in the subsequent annealing process [12]. Liu et al. reported that for a 6.2 wt% Si electrical steel with $C < 0.01$, hot rolling was beneficial to the final magnetic properties [16]. Xu et al. reported the beneficial effects of annealing prior to cold rolling on the electrical steel microstructure and magnetic properties [17].

Although there have already been some studies conducted that examine the influence of the rolling process on the NGO electrical steels [18–20], there are few studies about the influence of hot rolling on the thin strip produced by the TRSC process. Because the TRSC process can directly cast 2 mm thick strip, the process has the potential for producing NGO electrical steel laminations, with improved time and energy savings. Thus, it is worthwhile to study the influence of the rolling process on the NGO electrical steels with conditions that simulate the solidification conditions of the TRSC process.

In this study, Fe-3.3 wt% Si non-oriented electrical steel was produced using a vacuum assisted fast cooling sampling method to simulate the solidification conditions of the TRSC process. The influence of rolling deformation on the magnetic properties, grain growth, and texture are analyzed and discussed.

2 Materials and methods

2.1 Materials

Two non-oriented electrical steels with different carbon and sulfur content were melted in a coreless medium frequency induction furnace under an Argon protective atmosphere. Table 1 shows the chemical composition of these steels. Steel 1 was produced using a high carbon and sulfur (C&S) composition, while Steel 2 was produced using a low C&S chemistry to avoid the negative influences of precipitates and phase transformations on NGO Si steel magnetic properties. The low C&S composition is generally more suited to industrial NGO electrical steel production. Samples were directly taken from the induction furnace at 100 ºC superheat using a vacuum sampler, described in the following subsection.

2.2 Sampling method

In this study, a vacuum assisted fast cooling (VA) sampling method was used to take samples that simulate the solidification conditions of the TRSC process. As reported in previous studies, a vacuum assisted process is used to draw liquid steel into a thin internal cavity inside a copper mold [3, 21] to produce a strip sample with high solidification cooling rate. The as-cast samples were 2 mm thick. Figure 1a shows a schematic diagram of the VA sampler, and Fig. 1b shows an as-cast sample after solidification in the VA sampler.

2.3 Processing schedules

In this study, as-cast samples were thermo-mechanical treated, simulating the industrial TRSC process. Three thermo-mechanical processing routes were designed with different hot rolling (HR) deformations (0, 25 and 47%). After hot rolling, all samples were cold rolled to a final thickness of 0.35 mm. Thus, higher HR deformation resulted in lower CR deformation with a combined total HR + CR reduction from 2 to 0.35 mm thickness. After the rolling process, samples were batch annealed at 1050 ºC for various times (1, 6, 18 and 24 h). The schematic diagram of the thermo-mechanical processing route is shown in Fig. 2.

Table 1 Chemical composition of the studied 3.4 wt% Si steels (wt%)

Steels	C	Si	Mn	Al	S	P	Cr	N
High C&S	0.0098	3.44	1.48	0.002	0.0087	0.010	0.028	0.0074
Low C&S	0.0046	3.45	1.50	0.001	0.0038	0.008	0.030	0.0044

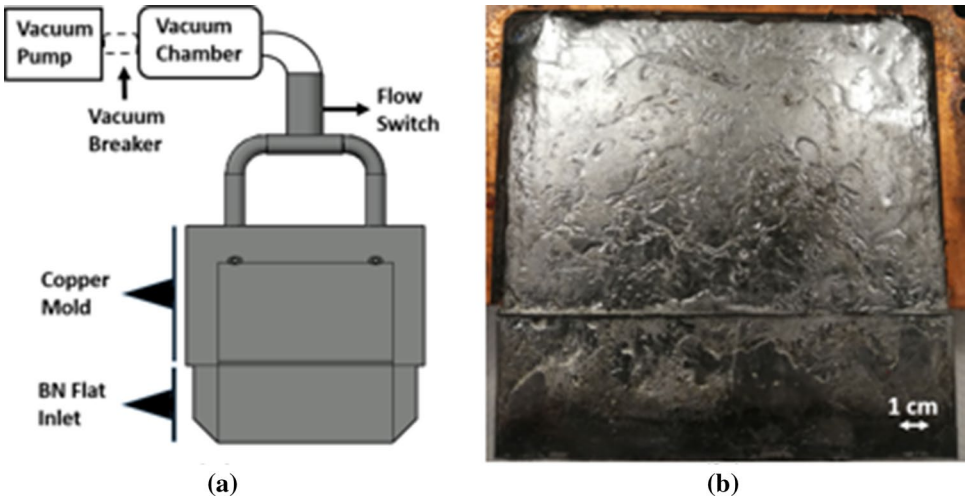

Fig. 1 **a** Schematic diagram of vacuum assisted fast cooling (VA) sampler, and **b** as-cast sample

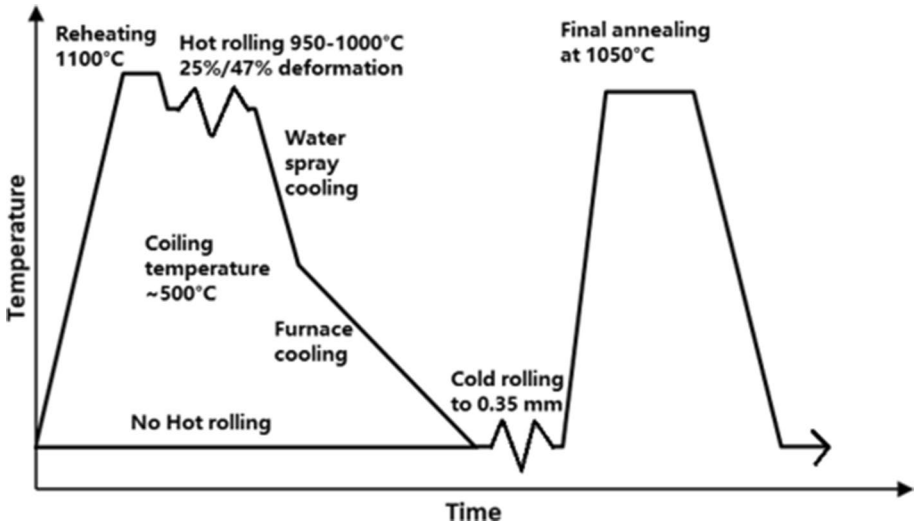

Fig. 2 Schematic diagram of thermo-mechanical processing route

2.4 Microstructure characterization and magnetic properties test

Samples were prepared metallographically, etched using water-based picric acid to reveal the dendrite structure and Nital etchant to reveal the grain structure. The linear intercept method according to ASTM E112–13 was used for performing the secondary dendrite arm spacing (SDAS) and grain size measurement [22].

The solidification cooling rate of the VA as-cast sample was calculated from the measured SDAS. Based on the expected cooling rate and the chemical composition, the Suzuki's equation was used for this calculation [23].

$$S_2 = 688(60 \times r)^{-0.36} \tag{1}$$

where S_2 is the SDAS in μm, and r is the solidification cooling rate in K/s.

The optimum grain sizes are used to minimize the core loss for different test conditions. This is because exceptionally coarse grain sizes can lead to higher permeability, lower coercivity, and large domain size, which in turn can increase the core loss [24]. De Campos [4] reported that the optimum grain size (G_{sOp}) can be described as follows:

$$G_{sOp} = \left(\frac{c\rho}{B^{0.4}t^2f^{1/2}}\right)^{2/3} \tag{2}$$

where c is an experimentally determined constant, ρ is the resistivity, B is the magnetic induction, t is the sample thickness, and f is the operating frequency.

Magnetic properties were measured using a single sheet tester, which is based on the ASTM A1036 [25].The test samples were prepared by cutting processed material into 100 mm long, 30 mm wide strips in the rolling direction. Core loss was measured at 50 and 60 Hz, 1.5 and 1.0 T

conditions ($P_{1.5/50}$, $P_{1.5/60}$, $P_{1.0/50}$, $P_{1.0/60}$). Magnetic induction was measured at 2500 and 5000 A/m conditions (B_{25}, B_{50}). The final recrystallized crystal orientations were analyzed using electron backscatter diffraction (EBSD) in a Helios SEM (30 kV, 11nA). Scans were conducted on the RD-ND (rolling direction—normal direction planes) cross section. The harmonic series expansion method was used in the orientation distribution function (ODFs) calculations.

3 Results and discussion

3.1 Solidification cooling rate

The dendrite structure of the VA as-cast sample is shown in Fig. 3. Using the linear intercept method, the SDAS was measured to be ~ 10 µm. Using Eq. (1), the solidification cooling rate was calculated to be ~ 1700 K/s, which is in the range reported for industry 2 mm thick strip TRSC process [26, 27].

The 0% HR (100% CR) processed sample is shown in Fig. 4a. As observed, many edge cracks propagated after the cold rolling process. This was caused by the residual stresses and microstructure of the steel, which formed based on the high solidification cooling rate. On the other hand, little to no edge cracking was observed during the processing of the 25% HR and 47% HR samples, as shown in Fig. 4b.

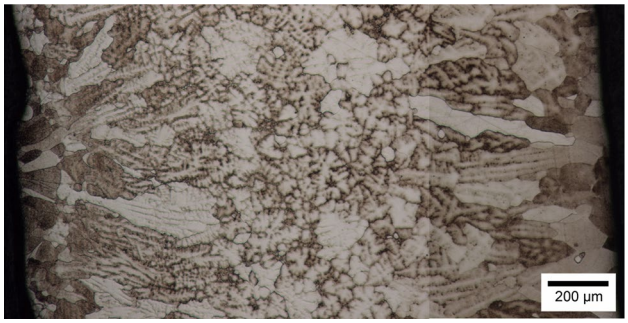

Fig. 3 Dendrite structure of the as-cast VA sample (etched by water-based picric acid)

3.2 Grain size

To minimize the core loss of 0.35 mm thick 3.3wt% Si NGO electrical steel (4.70×10^{-7} Ω·m) at 1.5 T and 50 Hz condition, Eq. (2) was used to calculate the optimum grain size, which was determined to be ~ 250 µm for the testing conditions. Thus, steel with a grain size close to 250 µm is expected to exhibit a decreased core loss at the 1.5 T and 50 Hz condition.

The average grain sizes after 1, 6, 18, 24 h batch annealing at 1050 °C are shown in Fig. 5. For the high C&S samples with 24 h annealing, with the increase of the HR deformation, the average grain size increased to 89, 148, and 190 µm. For low C&S samples with 24 h annealing, with the increase of the HR deformation, the average grain size increased to 136, 199, 249 µm. The measured average grain sizes were all smaller than the calculated optimum grain size. Among samples at the same HR deformation, the samples with lower C&S level showed coarser average grain sizes at each of the measured annealing times. Among the samples with similar C&S level, the samples with higher HR deformation showed coarser average grain sizes at each of the measured annealing time (Sample 47% HR > Sample 25% HR > Sample 0% HR).

For samples with high C&S levels, the final grain size was influenced by the α–γ phase transformation during the annealing process which likely retarded grain boundary migration. It is reported that for the 3.3 wt% Si steel, there is no austenite when carbon is less than 0.02 wt%. With 0.036 wt% C, after 1 h annealing at 1000 °C, ~ 12% austenite estimated to be present [12]. Furthermore, the presence of austenite during hot deformation has been reported to increase the recrystallization rate during subsequent annealing and reduce the recrystallized grain size [12]. Among samples with different HR deformation, the increased HR processing resulted in less cold reduction which reduces dislocation

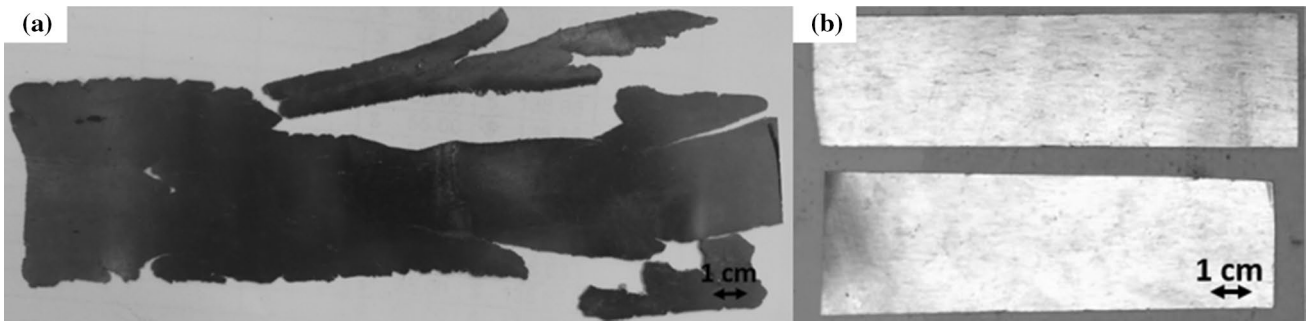

Fig. 4 VS sample been hot rolled and cold rolled to 0.35 mm **a** No HR sample, **b** 25% (top) and 47% (bottom) HR sample

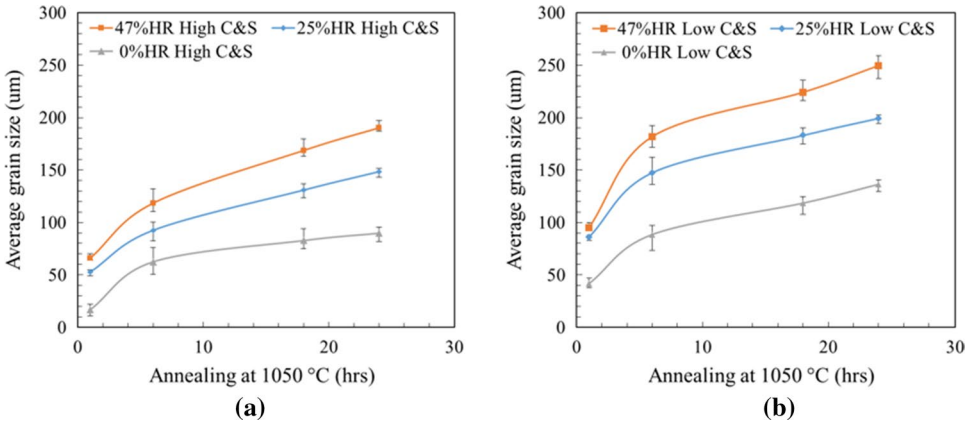

Fig. 5 Average grain size after batch annealing at 1050 °C for **a** High C&S samples, and **b** Low C&S samples

density and decreases the number of nucleation sites in subsequent recrystallization process, favoring coarser grains.

3.3 Magnetic properties

Because the measured average grain sizes were all smaller than the calculated optimum grain size, the best magnetic properties were expected to be observed with the 24 h annealed samples. The magnetic properties were measured on samples processed at 1050 ºC with 24 h batch annealing. Measured results are shown in Table 2. For all C&S levels, the 25 and 47% HR final annealed samples all met the magnetic properties requirement for the 35W250 NGO electrical steel at GB/T 2521.1, which is 2.50 W/kg for $P_{1.5/50}$ [28].

In general, samples processed at higher HR deformation (with same chemical composition), and the samples with lower C&S level (with same HR deformation) show better magnetic properties. The results are directly related to the average grain size that was discussed previously. Comparing magnetic property and average grain size results in Table 2, larger grain size is helpful to decrease the core loss. The only exception was the samples with 25% HR. Although the low C&S sample had a coarser average grain size than the sample with high C&S, they show similar core loss at 1.5 T test condition.

Based on the inclusion analysis reported in a previous study [21], VA samples all had a similar inclusion size distribution. Thus, other than the grain size differences that were discussed previously, the magnetic properties are also influenced by texture, which will be discussed in the following subsection.

3.4 Texture effect

Figure 6 shows the typical textures expected in the ODF section of fully processed electrical steel samples, while Figs. 7 and 8 reveals the evolutionary texture intensities and patterns influenced by the rolling process. The Cube {100}⟨001⟩, Brass {110}⟨112⟩, Goss {110}⟨001⟩ are the main orientations obtained in these ODF images results. The main texture fraction evolution with HR deformation is shown in Fig. 9.

For the high C&S samples, increasing the HR deformation showed a decrease in the intensities of Goss orientation. There are high intensities of Cube orientation on the sample with 47% HR, while there are less on the sample with 25% HR and 0% HR. The γ-fiber has disappeared in each of the

Table 2 Magnetic properties after final annealing

	$P_{1.5/50}$ (W/kg)	$P_{1.5/60}$	$P_{1.0/50}$ (W/kg)	$P_{1.0/60}$	B_{25} mT	B_{50}	Average grain size μm
High C&S (0% HR)	2.90	3.67	1.38	1.73	1672	1782	90
High C&S (25% HR)	2.38	3.05	1.18	1.49	1860	1999	148
High C&S (47% HR)	2.27	2.87	1.08	1.36	1970	2096	190
Low C&S (0% HR)	2.79	3.52	1.35	1.69	1786	1924	136
Low C&S (25% HR)	2.38	3.05	1.13	1.45	1910	2079	199
Low C&S (47% HR)	2.02	2.59	0.95	1.22	1990	2109	249

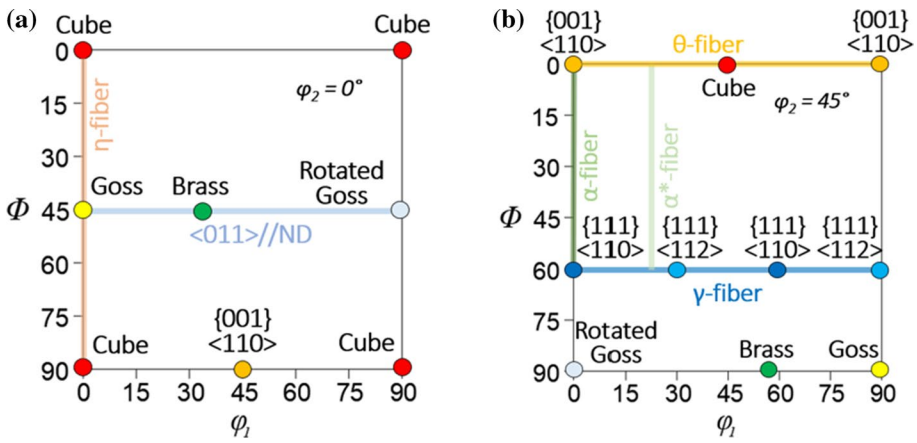

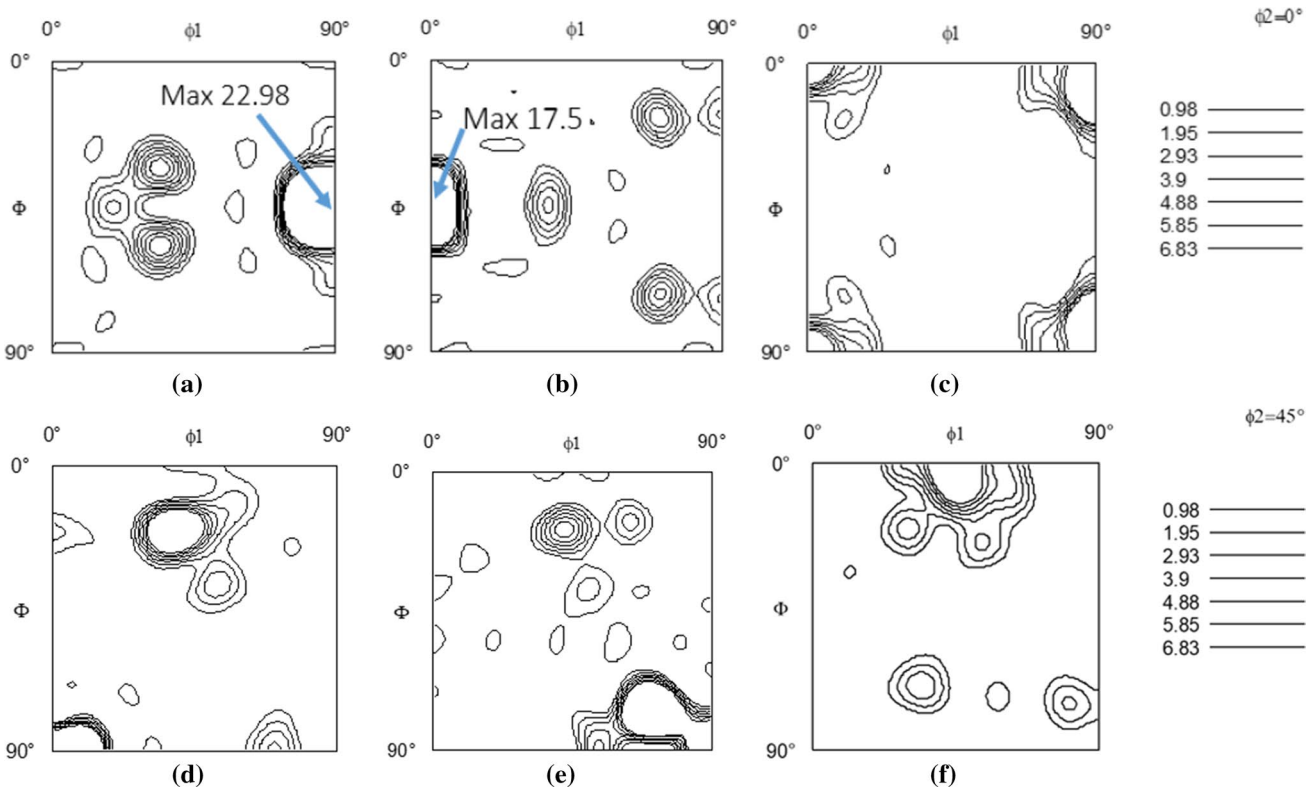

Fig. 6 Typical textures in the electrical steel, displayed in **a** $\varphi_2=0°$, and **b** $\varphi_2=45°$ ODF section

Fig. 7 ODF map displayed at $\varphi_2=0°$ section of the final annealed high C&S strip sample with **a** 0% HR, **b** 25% HR, **c** 47% HR, and ODF map displayed at $\varphi_2=45°$ section with **d** 0% HR, **e** 25% HR, **f** 47% HR

samples after annealing, which is beneficial to the magnetic properties. Compared to γ-fiber texture, the Cube and Goss textures are more ideal for magnetic properties [29].

For the low C&S samples, a rotated Goss orientation is observed in each of the samples. On the sample with 0% HR, there are low intensity Cube orientations and some rotated Goss orientations. This 0% HR sample is highly influenced by the presence of γ-fiber formed during the cold rolling process, while it is absent in the samples with 25% HR and 47% HR.

The recrystallization textures after final annealing are highly influenced by the deformation structure and texture during the rolling process. The strain induced boundary migration (SIBM) and subgrain growth at grain boundaries are considered to be the principal mechanisms for grain nucleation [13]. The subgrain growth is usually observed in <111> //ND (γ-fiber) deformed grain, while the nucleation by SIBM always happens in <100> //ND (θ-fiber) deformed grain. When samples were hot rolled before CR processing, the proportion of shear bands was decreased

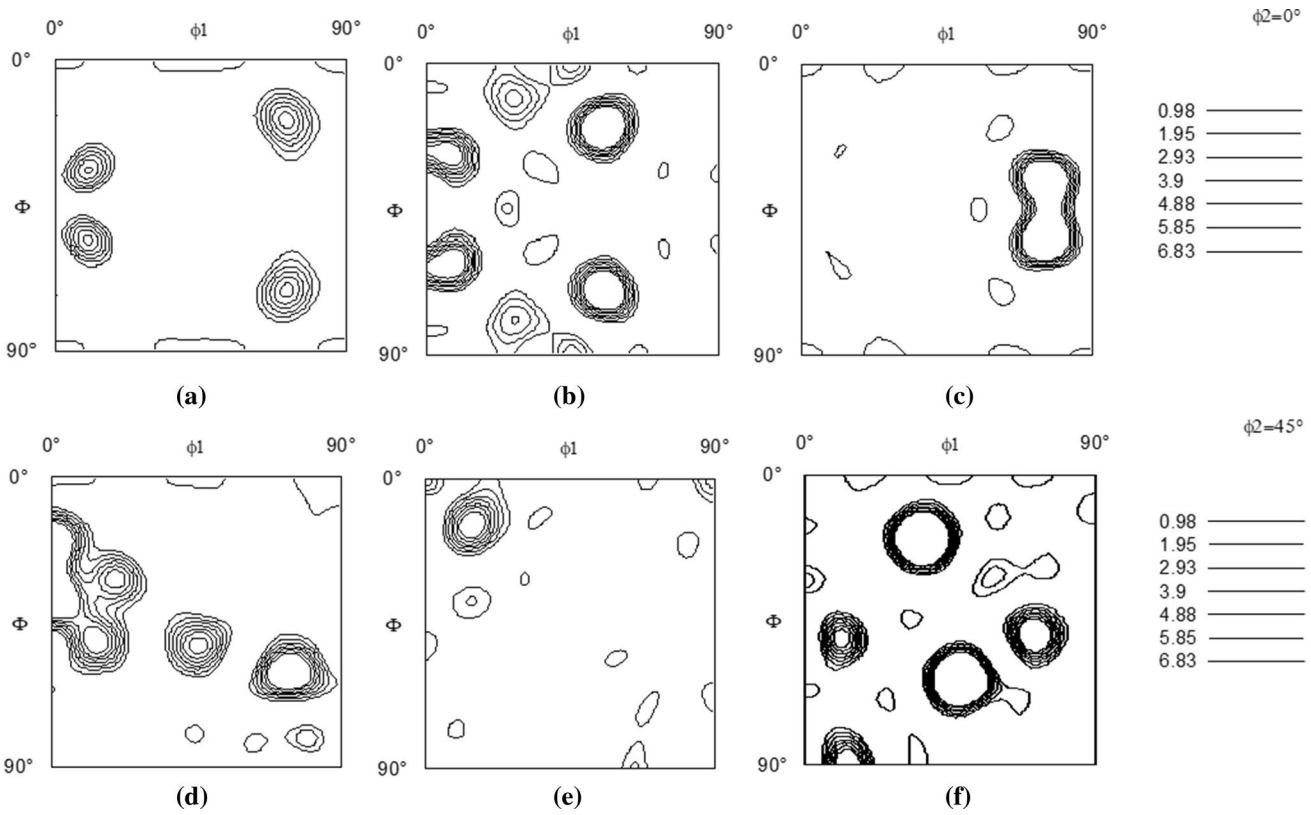

Fig. 8 ODF map displayed at $\varphi_2 = 0°$ section of the final annealed low C&S strip sample with **a** 0% HR, **b** 25% HR, **c** 47% HR, and ODF map displayed at $\varphi_2 = 45°$ section with **d** 0% HR, **e** 25% HR, **f** 47% HR

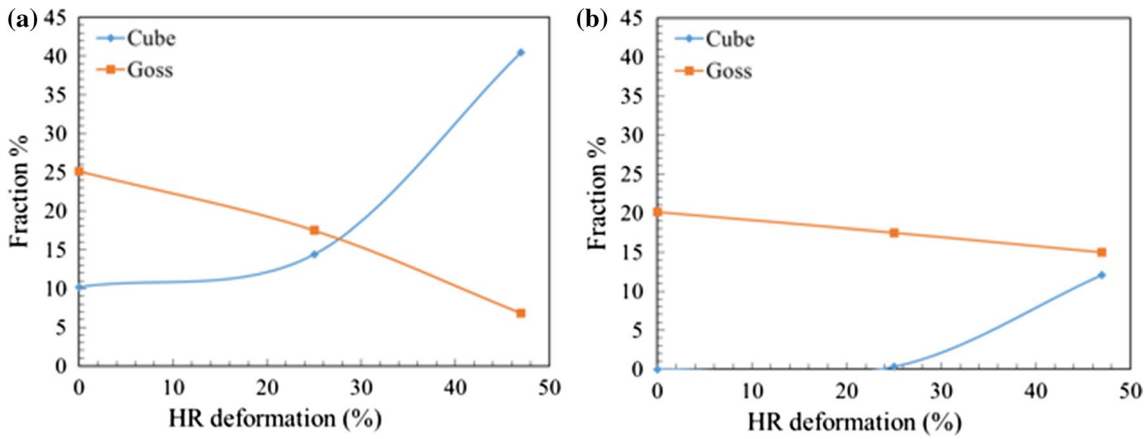

Fig. 9 Volume fractions of the main textures vs HR deformation: **a** High C&S VA sample, **b** Low C&S VA sample

while the retention of {100} deformation microstructure was enhanced [13].

Among samples at 25% HR deformation, the sample with high C&S shows a higher intensity of Goss orientations, while the intensity of the Cube texture is lower on the sample with low C&S. This appears to explain why at 25% HR deformation, despite the fact that the grain size of low C&S

sample is coarser, it has similar core loss results compared to the high C&S sample at 1.5 T condition.

4 Conclusion

In this study, Fe-3.3 wt% Si non-oriented electrical steel strip samples were produced in the lab to simulate the solidification conditions of the TRSC process. Thermo-mechanical processing routes with 0% HR, 25% HR, and 47% HR were studied on samples with high and low C&S. The measured magnetic properties of the fully processed 25% HR and 47% HR samples all met the requirements for 35W250 NGO electrical steel in GB/T 2521.1, which is 2.50 W/kg for $P_{1.5/50}$. For the samples with the same HR deformation, the low C&S samples were observed to have a coarser average grain size after final annealing. It is likely that the high C&S samples were influenced by an γ–α phase transformation occurring during recrystallization annealing and the presence of austenite during hot deformation process. With an increase of the HR deformation, the average grain size after final annealing was also increased. This coarser grain size also led to lower core loss ($P_{1.5/50}$, $P_{1.5/60}$, $P_{1.0/50}$, $P_{1.0/60}$) and higher magnetic induction (B_{25}, B_{50}). Samples at 25% HR with low C&S and high C&S show similar core loss (1.5 T condition) results despite the fact that the grain size in the former is coarser than in the latter. It is influenced by difference on texture. For the final annealed sample with high C&S, the intensities of Goss orientation were decreased with an increase in HR deformation. This observation is considered to be influenced by the decreased proportion of shear bands.

The phenomenon observed in this study also verified some results published by others obtained on TRSC non-oriented electric steel. For example, with the increase of HR deformation (decrease of CR deformation), Goss texture fraction decreased. Jiao also reported similar finding to the 3.0% Si non-oriented electric steel 67 ~ 83% CR deformation range [30].

Acknowledgements This research was performed at Missouri University of Science and Technology (Missouri S&T). The authors would like to thank the graduate research assistants in MSE for their assistance during casting trials and acknowledge Brian Bullock for his help with the setup and manufacture of the samplers. This project was supported by Nucor Corporation and Castrip LLC, so special thanks go to all of their help and guidance. The authors are also grateful to all the faculties and industry mentoring committee of Peaslee Steel Manufacturing Research Center (PSMRC) at Missouri University of Science and Technology (Missouri S&T) for their help and guidance.

References

1. Y. Oda, T. Okubo, M. Takata, Recent development of non-oriented electrical steel in JFE steel. JFE Tech. Rep. **21**, 7–13 (2016)
2. J. Hong, H. Choi, S. Lee, J.K. Kim, Y.M. Koo, Effect of Al content on magnetic properties of Fe-Al non-oriented electrical steel. J. Magn. Magn. Mater. **439**, 343–348 (2017)
3. Y. Du, R.J. O'Malley, M.F. Buchely, M. Xu., Design and evaluation of a lab size vacuum sampling method for simulating the twin-roll strip casting process, in *AISTech - Iron and Steel Technology Conference Proceedings* vol. 2021-June, pp 483–490, 2021, https://doi.org/10.33313/382/048.
4. M.F. De Campos, J.C. Teixeira, F.J.G. Landgraf, The optimum grain size for minimizing energy losses in iron. J. Magn. Magn. Mater. **301**(1), 94–99 (2006)
5. G. Ouyang, X. Chen, Y. Liang, C. Macziewski, J. Cui, Review of Fe-6.5 wt% Si high silicon steel—a promising soft magnetic material for sub-kHz application. J. Magn. Magn. Mater. **481**, 234–250 (2019)
6. J.-T. Park, J.A. Szpunar, Effect of initial grain size on texture evolution and magnetic properties in nonoriented electrical steels. J. Magn. Magn. Mater. **321**(13), 1928–1932 (2009)
7. Y. Lu et al., Investigation of microstructure and properties of strip-cast 4.5 wt% Si non-oriented electrical steel by different rolling processes. J. Magn. Magn. Mater. **497**, 165975 (2020)
8. H. Jiao et al., Texture evolution in twin-roll strip cast non-oriented electrical steel with strong cube and Goss texture. Acta Mater. **199**, 311–325 (2020)
9. N. Shan, J. Liu, Y. Sha, F. Zhang, L. Zuo, Development of through-thickness cube recrystallization texture in non-oriented electrical steels by optimizing nucleation environment. Metall. Mater. Trans. A. **50**(5), 2486–2494 (2019)
10. S.H. Lee, D.N. Lee, Analysis of deformation textures of asymmetrically rolled steel sheets. Int. J. Mech. Sci. **43**(9), 1997–2015 (2001)
11. J.-T. Park, J.A. Szpunar, Evolution of recrystallization texture in nonoriented electrical steels. Acta Mater. **51**(11), 3037–3051 (2003)
12. S. Akta, G.J. Richardson, C.M. Sellars, Hot deformation and recrystallization of 3% silicon steel part 1: microstructure, flow stress and recrystallization characteristics. ISIJ Int. **45**(11), 1666–1675 (2005)
13. H. Jiao et al., Influence of hot deformation on texture and magnetic properties of strip cast non-oriented electrical steel. J. Magn. Magn. Mater. **462**, 205–215 (2018)
14. J.S.M. Pedrosa, S. da Costa Paolinelli, A.B. Cota, Influence of initial annealing on structure evolution and magnetic properties of 3.4% Si non-oriented steel during final annealing. J. Magn. Magn. Mater. **393**, 146–150 (2015)
15. M. Atake, M. Barnett, B. Hutchinson, K. Ushioda, Warm deformation and annealing behavior of iron–silicon–(carbon) steel sheets. Acta Mater. **96**, 410–419 (2015)
16. H.-T. Liu, Z.-Y. Liu, Y.-Q. Qiu, Y. Sun, G.-D. Wang, Microstructure, texture and magnetic properties of strip casting Fe–6.2 wt% Si steel sheet. J. Mater. Process. Technol. **212**(9), 1941–1945 (2012)
17. Y. Xu et al., Effect of pre-annealing prior to cold rolling on the precipitation, microstructure and magnetic properties of strip-cast non-oriented electrical steels. J. Mater. Sci. Technol. **33**(12), 1465–1474 (2017)
18. E. Gomes, J. Schneider, K. Verbeken, H. Hermann, Y. Houbaert, Effect of hot and cold rolling on grain size and texture in Fe-Si strips with Si-content larger than 2 wt%. Mater. Sci. Forum **638**, 3561–3566 (2010)
19. W.C. Jeong, Effect of hot-rolling temperature on microstructure and texture of an ultra-low carbon Ti-interstitial-free steel. Mater. Lett. **62**(1), 91–94 (2008)
20. H.-Z. Li et al., Effects of warm temper rolling on microstructure, texture and magnetic properties of strip-casting 6.5 wt% Si electrical steel. J. Magn. Magn. Mater. **370**, 6–12 (2014)

21. Y. Du, Effect on cooling rate on magnetic properties of Fe-3.4 wt% Si Non-oriented electrical steel, *Manuscript submitted for publication*, 2021.
22. ASTM E112–13 Standard Test Methods for Determining Average Grain Size (ASTM International, West Conshohocken, 2013).
23. A. Suzuki, T. Suzuki, Y. Nagaoka, Y. Iwata, On secondary dendrite arm spacing in commercial steels having different carbon contents. Nippon Kinzoku Gakkai-Si **32**(12), 1301–1305 (1968)
24. J. Füzer et al., Investigation of total losses of non-oriented electrical steels. Acta Physica Polonica-Ser. A Gen. Phys. **118**(5), 1018 (2010)
25. ASTM A1036 - 04(2020) Standard guide for measuring power frequency magnetic properties of flat-rolled electrical steels using small single sheet testers (ASTM International, West Conshohocken, 2020).
26. P. Campbell, W. Blejde, R. Mahapatra, R. Wechsler, Recent progress on commercialization of Castrip® direct strip casting technology at Nucor Crawfordsville. Metallurgist **48**(9–10), 507–514 (2004)
27. R. Wechsler and P. Campbell, The first commercial plant for carbon steel strip casting at Crawfordsville, in *Dr. Manfred Wolf Symposium*, 2002, pp. 70–79.
28. GB/T 2521.1–2016 Cold-rolled electrical steel delivered in the fully-processed state - Part 1: Grain non-oriented steel strip(sheet).
29. J.J. Sidor, K. Verbeken, E. Gomes, J. Schneider, P.R. Calvillo, L.A.I. Kestens, Through process texture evolution and magnetic properties of high Si non-oriented electrical steels. Mater. Charact. **71**, 49–57 (2012)
30. H. Jiao et al., High-permeability and thin-gauge non-oriented electrical steel through twin-roll strip casting. Mater. Des. **136**, 23–33 (2017)